論文 한국정밀공학회지 제12권 제10호 1995. 10
Journal of the Korean Society of Precision Engineering Vol.12. No.10. October. 1995.

이중 경계적분방정식에 의한 크랙 문제의 해석

윤 승 원,* Thomas J. Rudolphi**

On Dual Boundary Integral Equations for Crack Problems

Seungwon Youn,* Thomas J. Rudolphi**

ABSTRACT

선형 탄성 등방성 물체 내에 있는 일반적인 복합모드 크랙 문제들을 해석하기 위한 이중 경계적분방정식의 일반식과 계산해법이 제시되었다. 크랙면이 포함된 물체 해석에 있어서 유일한 해를 얻기 위하여, 한 면상의 점에는 변위 경계적분방정식이 적용되었고 마주하고 있는 상대면 상의 점에는 인력 경계적분방정식이 적용되었다. 인력 및 변위 경계적분방정식의 강특이해 및 초특이해 적분항들은 수치해법을 적용하기 전에 정상화되었다. 정상화 과정 중 보정되는 강특이적분항이 상대 크랙면 상의 특이해 요소를 따라 직접 적분되는 것을 격리시키기 위하여, 특이해 적분 경로를 완만한 곡면으로 우회시킨 가상의 비특이해 보조경계로 대치하여 적분값을 계산하였다. 제시된 해법의 정확성과 효율성을 예시하기 위하여, 2차원 및 3차원 크랙 문제의 변형 후 모습과 응력강도계수 계산 결과를 보였다.

Key Words : Boundary Integral Equation, Hypersingular Singularity, Mixed-Mode Crack, Integral Identity, Singular Integrals, Regularization, Auxiliary Surface, Stress Intensity Factors

1. Introduction

Most elastostatic problems can be solved using only the displacement boundary integral equations (DBIE's)which are determined by the limit forms of the Somigliana's identity or the displacement representation. In crack problems, when the upper and lower crack surfaces lie in the same location, the collocation point on one crack surface occupies the same spatial coordinates as the opposite crack surface. In this case, the DBIE's are degenerated. Two collocation points in the same plane generate the same equation and leads to a singular coefficient matrix for the system. For this reason, closed crack problems cannot be solved by the use of the DBIE's alone when the body is modelled with a single region.

* 생산기술연구원 생산시스템개발센터(종신회원)
** Iowa State University, Department of Aerospace Engineering and Engineering Mechanics

To overcome the singularity problem in overlapping crack surfaces, several special techniques have been developed. These include the displacement discontinuity method[1], the specialized Green's function method[2], the multidomain method[3] and the dual integral equation method[4]. the drawback of a multidomain method is non-uniqueness of the artificial boundary in modelling and a larger system of equations than needed.

To solve a general mixed-mode crack without the special techniques mentioned above, one needs another integral equation in addition to the DBIE's to ensure a unique solution. Formed by linear combinations of derivatives of the DBIE's through Hooke's law, the traction boundary integral equations(TBIE's) have been shown to provide the additional equations. Guidera and Lardner[5]have first used the TBIE's explicitly to solve the problem of a penny-shaped crack subjected to the arbitrary tractions in an infinite medium. The DBIE's and the TBIE's are herein referred to as dual boundary integral equations.

The fundamental solutions of the DBIE's contain both weak and strong(Cauchy)singularities and can be integrated in the sense of improper integrals and as Cauchy principal value integrals. However, the fundamental solution kernels associated with the TBIE's have both strong(Cauchy)and stronger, termed hypersingular singularities, due to the differentiation process. The hypersingular kernels in the TBIE's cause some difficulties in the numerical implementation. To reduce the singularity order of the hypersingular integrals, Cruse and Vanburen[6] subtracted the first term of a Taylor expansion from the density (displacement)function. They also derived some integral identities for the stress tensor at points on the surface by considering a rigid body translation. Similarly, Jeng and Wexler[7] and Aliabadi et al.[8] subtracted the first term of a Taylor expansion. In either case, the added back terms are still hypersingular and remain to be computed. Brandao[9] and Kaya and Erdogan[10] subtracted the first two terms of a Taylor expansion to evaluate one-dimensional hypersingular integrals in the Hadamard sense. For multi-dimensional problems, Krishnasamy et al.[11] also subtracted the first two terms of a Taylor expansion to regularize the hypersingular integrals.

Recently, many researchers have contributed to the use of the hypersingular boundary integral equations[11~15]. Some important identites pertaining to the fundamental solutions were established by Rudolphi et al. [16 17] and have been used to avoid the stronger integrals. The regularization process using a Taylor expansion and the identities pertaining to the fundamental solutions to get regularized form of the boundary integral equation has become a popular method. The added back terms which appear during the requlariza-tion process are replaced by weakly singular integrals through the pertinent identities. These identities can be used to avoid one hypersingular integral, but in crack problems there are always two such integrals to regularize, one on each crack surface. As a part of what they called the modal solution method(which is the same as the above mentioned identities), Lutz et al.[18] have constructed tent-like closure surfaces and used the integral idetities on both crack surfaces. Portela et al.[19] and Mi and Aliabadi[20] solved two- and three-dime-nsional closed crack problems by the dual boundary integral equations, respectively. After the regularization with the key terms of a Taylor expansion, they have integrated the finite part integrals, the stronger singularities, in the TBIE's on a vanishingly small part of the boundary near the limit point following the technique Guig-

giani et al.[15]

In this work, the computational algorithm for the solution of general mixed-mode crack problems in a linearly elastic isotropic medium, in bounded or unbounded domains, in two- and three-dimensions has been developed by use of the dual boundary integral equation approach, together with the auxiliary surface. The displacement representation is derived by Betti's reciprocal work theorem. By taking the derivatives of the displacement representation and by contracting on the elastic moduli as required by Hooke's law, the traction representation is formed. By presuming the density functions are sufficiently continuous at the singular point, the displacement and the traction representations are regularized by subtracting and adding back the key terms of the Taylor expansion to the density function and the relevant integral identities. During the regularization process, the whole integration range is divided into two, that is, a singular part and the remainder, for convenience. By taking the limit of the source point from the interior to the surface, the DBIE's and the TBIE's are formed from each of regularized representations. The regularized boundary integral equations have, at most, weakly singular integrals.

The added back integrals contain the hypersingular kernels on both crack surfaces. To integrate these added back singular integrals, the integration is carried out over smoothly curved auxiliary surfaces that replace the actual singular surface.[22] The introduced auxiliary surfaces always provide non-singular integration paths and result modified forms of identities for uncracked bodies. The developed computational forms of the DBIE's and the TBIE's have all similar features. For the numerical integration, the usual Gaussian quadrature technique is used.

As examples, each one of typical two- and three-dimensional mixed-mode crack model is analyzed. Crack tip stress intensity factors are determined from the nodal displacements on the crack surfaces and comparison to known analytic solutions is made.

2. Representations for Elastostatics

As a starting point, the well-known Somigliana's identity or the displacement representation is derived from the governing equation in elasticity and Betti's reciprocal work theorem with the known fundamental solutions as

$$u_i(\vec{\xi}) = \int_S U_{ij}(\vec{x},\vec{\xi}) t_j(\vec{x}) dS(\vec{x}) - \int_S T_{ij}(\vec{x},\vec{\xi}) u_j (\vec{x}) dS(\vec{x}) + \int_V U_{ij}(\vec{X},\vec{\xi}) f_j(\vec{X}) dV(\vec{X}) \quad (1)$$

where the point $\vec{x}$ is on the boundary and the points $\vec{\xi}$ and $\vec{X}$ are in the internal and on the boundary. Somigliana's identity is valid for points in the domain V, including the boundary S, when u_i and t_i are known at every boundary point. The displacement components at any point in the field and on the surface can be obtained from the boundary values u_j and t_j, the body forces f_j and the fundamental solutions.

The stresses can be obtained by taking the derivatives of Somigliana's identity with respect to the coordinates ξ_k and by contracting the material property E_{pqik} on the derivatives as

$$\frac{\partial u_i(\vec{\xi})}{\partial \xi_k} = \int_S \frac{\partial U_{ij}}{\partial \xi_k} t_j(\vec{x}) dS(\vec{x}) - \int_S \frac{\partial T_{ij}}{\partial \xi_k} u_j(\vec{x}) dS(\vec{x}) + \int_V \frac{\partial U_{ij}}{\partial \xi_k} f_j(\vec{X}) dV(\vec{X}) \quad (2)$$

with the regularized form of Hooke's law given by

$$\sigma_{pq}(\vec{\xi}) = E_{pqik}\frac{\partial u_i(\vec{\xi})}{\partial \xi_k} \tag{3}$$

the stresses can be obtained from the following.

$$\sigma_{pq}(\vec{\xi}) = \int_S E_{pqik}\frac{\partial U_{ij}}{\partial \xi_k} t_j(\vec{x})dS(\vec{x}) - \int_S E_{pqik}\frac{\partial T_{ij}}{\partial \xi_k} u_j (\vec{x})dS(\vec{x}) + \int_V E_{pqik}\frac{\partial U_{ij}}{\partial \xi_k} f_j(\vec{X})dV(\vec{X}) \tag{4}$$

Note that the derivatives of the fundamental solution kernels in equation(4) have higher order singularities than in the displacement representation.

By defining two new variables

$$\Sigma_{jpq} = E_{pqik}\frac{\partial U_{ij}(\vec{x},\vec{\xi})}{\partial \xi_k} \tag{5}$$

$$\Theta_{jpq} = E_{pqik}\frac{\partial T_{ij}(\vec{x},\vec{\xi})}{\partial \xi_k} \tag{6}$$

one can calculate the stresses at any point in the interior and on the boundary from

$$\sigma_{pq}(\vec{\xi}) = \int_S \Sigma_{jpq} t_j(\vec{x})dS(\vec{x}) - \int_S \Theta_{jpq} u_j(\vec{x})dS(\vec{x}) + \int_V \Sigma_{jpq} f_j(\vec{X})dV(\vec{X}) \tag{7}$$

The Cauchy's stress formula with the material properties for the traction components at any point $\vec{\xi}$ on a plane with normal $\vec{\nu}$ may be written as

$$t_p(\vec{\xi}) = E_{pqik}\nu_q(\vec{\xi})\frac{\partial u_i(\vec{\xi})}{\partial \xi_k} \tag{8}$$

By contracting the normal vector components $\nu_q(\vec{\xi})$ at $\vec{\xi}$ on the stresses components (7), one has the following traction representation.

$$t_p(\vec{\xi}) = \int_S \Sigma_{jpq}\nu_q(\vec{\xi})t_j(\vec{x})dS(\vec{x}) - \int_S \Theta_{jpq}\nu_q(\vec{\xi})u_j (\vec{x})dS(\vec{x}) + \int_V \Sigma_{jpq}\nu_q(\vec{\xi})f_j(\vec{X})dV(\vec{X}) \tag{9}$$

By defining the following two variables

$$U^*_{pj} = \Sigma_{jpq}\nu_q(\vec{\xi}) \tag{10}$$

$$T^*_{pj} = \Theta_{jpq}\nu_q(\vec{\xi}) \tag{11}$$

one gets the compact form of the traction representation as

$$t_p(\vec{\xi}) = \int_S U^*_{pj} t_j(\vec{x})dS(\vec{x}) - \int_S T^*_{pj} u_j(\vec{x})dS(\vec{x}) + \int_V U^*_{pj} f_j(\vec{X})dV(\vec{X}) \tag{12}$$

where U^*_{pj} contains the derivatives of U_{ij} and T^*_{pj} contains the derivatives of T_{ij} with respect to ξ_k, together with the elastic constants and the normal vector components $\vec{\nu}$.

One can see that the traction representation (12) is the derivative form of the displacement representation and has a form similar to equation(1). Equation (12) gives one an additional independent integral representation to solve many engineering problems together with the displacement representation.

As the source point goes the field point, $r \to 0$, all fundamental solution kernels contained in the displacement representation and the traction representation become singular. The weakly singular kernels, $O(\ln r)$ in 2-D and $O(1/r)$ in 3-D, can be integrated by a coordinate transformation method. The integrals for the strongly singular kernels, $O(1/r)$ in 2-D and $O(1/r^2)$ in 3-D, can be obtained through a surface exclusion and a Cauchy principal value interpretation. The hypersingular kernels, $O(1/r^2)$ in 2-D and $O(1/r^3)$ in 3-D, contained in the traction representation have been poorly understood and special techniques are required to integrate them numerically.

3. Identities for the Fundamental Solutions

By imposing the rigid body translation and the constant strain field solutions onto the

displacement or the traction representation, some important integral identities pertaining to the fundamental solutions are formed[6,16,17].

(1) *The first kind identity* is obtained from the displacement representation by considering the rigid body translation fields.

$$\int_S T_{ij}(\vec{x},\vec{\xi})dS = \begin{cases} -\delta_{ij} & (\vec{\xi}\in S\cup V) \\ 0 & (\vec{\xi}\in S\cup E) \end{cases} \quad (13)$$

From the first kind identity, one can obtain several modified identities by introducing an auxiliary boundary to the domain. With the partitioned integration ranges $S = S' + S_o$ or $S = \Gamma_o + S_o$ as shown in Fig.1, the first kind identity may be written as

$$\int_{S'+S_o} T_{ij}(\vec{x},\vec{\xi})dS = \begin{cases} -\delta_{ij} & (\vec{\xi}\in S\cup V) \\ 0 & (\vec{\xi}\in S\cup E) \end{cases} \quad (14)$$

$$\int_{\Gamma_o+S_o} T_{ij}(\vec{x},\vec{\xi})dS = \begin{cases} -\delta_{ij} & (\vec{\xi}\in S\cup V) \\ 0 & (\vec{\xi}\in S\cup E) \end{cases} \quad (15)$$

By subtracting equation (14) from (15) for the interior or the exterior domain respectively, one gets a unified identity for the first kind identity valid for the interior and the exterior domains, in the form

$$\int_{S'} T_{ij}(\vec{x},\vec{\xi})dS = \int_{\Gamma_o} T_{ij}(\vec{x},\vec{\xi})dS \quad (\vec{\xi}\in S\cup V\cup E) \quad (16)$$

(2) *The second kind identity* is obtained from the traction representation by considering the rigid body translation fields.

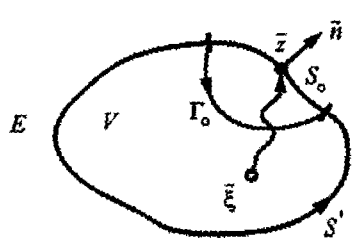

g. 1 The domain and an auxiliary boundary Γ_o

$$\int_S T_{ij}^*(\vec{x},\vec{\xi})dS = 0 \quad (\vec{\xi}\in S\cup V\cup E) \quad (17)$$

One can rewrite equation (17) by an auxiliary boundary as

$$\int_{S'} T_{ij}^*(\vec{x},\vec{\xi})dS = \int_{\Gamma_o} T_{ij}^*(\vec{x},\vec{\xi})dS = -\int_{S_o} T_{ij}^*(\vec{x},\vec{\xi})dS \quad (\vec{\xi}\in S\cup V\cup E) \quad (18)$$

(3) *The third kind identity* is obtained from the traction representation by considering the constant strain fields and applying the first kind identity.

$$\int_S T_{pj}^* r_k dS = \int_S E_{jqik}[U_{pj}^* n_q(\vec{x})dS + T_{pj}^* \nu_q(\vec{\xi})]dS \quad (19)$$

4. Dual Boundary Integral Equations Formulation

One may rewrite the displacement representation (1), by ignoring body force term, as

$$u_i(\vec{\xi}) + \int_S T_{ij}(\vec{x},\vec{\xi})u_j(\vec{x})dS(\vec{x}) = \int_S U_{ij}(\vec{x},\vec{\xi})t_j(\vec{x})dS(\vec{x}) \quad (20)$$

To remove the strong singularity in T_{ij} kernel, one can subtract and add back the first term of a Taylor expansion of the density function $\vec{u}$.

$$u_i(\vec{\xi}) + \int_S T_{ij}[u_j(\vec{x}) - u_j(\vec{\xi})]dS + \int_S T_{ij}dS u_j(\vec{\xi}) = \int_S U_{ij}t_j(\vec{x})dS \quad (21)$$

By applying the first kind identity for the interior, one obtains regularized displacement representation $\vec{u}$.

$$\int_S T_{ij}[u_j(\vec{x}) - u_j(\vec{\xi})]dS = \int_S U_{ij}t_j(\vec{x})dS \quad (22)$$

Now, let $\bar{\xi}$ go to $\vec{z}$ from the interior to the boundary as shown in Fig.1 by the limiting process to form the regularized displacement boundary integral equation.

$$\int_S T_{ij}[u_j(\vec{x}) - u_j(\vec{z})]dS = \int_S U_{ij} t_j(\vec{x}) dS \quad (\vec{x}, \vec{z} \in S) \tag{23}$$

For the exterior domain, by applying the exterior identity of (13) and by taking the limit $\bar{\xi} \to \vec{z}$, one gets identical result to the interior(23). Now, all variables in the DBIE's are on the boundary and the left-side integral has $O(1)$ singularity and is integrable in the ordinary sense. Here, the right-side integral is in the sense of a Cauchy principal value.

By subtracting two terms of a Taylor expansion to regularize the kernel, using the identities on the added back terms, and taking the limit $\bar{\xi} \to \vec{z}$, the TBIE's can be formulated similar to the displacement representation. Finally, one will have at most weakly singular integrals in the TBIE's. By considering the first kind identify for the interior, the TBIE's (12), by ignoring body force term, can be proceed as

$$t_p(\bar{\xi}) = \delta_{pj} t_j(\bar{\xi}) = -\int_S T_{pj}(\vec{x}, \bar{\xi}) dS t_j(\bar{\xi})$$

$$= -\int_S T_{pj}(\vec{x}, \bar{\xi}) t_j(\bar{\xi}) dS \tag{24}$$

$$\int_S T^*_{pj} u_j(\vec{x}) dS(\vec{x}) = \int_S \left[U^*_{pj} t_j(\vec{x}) + T^*_{pj} t_j(\bar{\xi}) \right] dS(\vec{x}) \tag{25}$$

By subtracting the first two terms of a Taylor expansion from $u(\vec{x})$ on the left side of equation(25), one gets

$$\int_S T^*_{pj} u_j(\vec{x}) dS(\vec{x})$$

$$= \int_S T^*_{pj} \left[u_j(\vec{x}) - u_j(\bar{\xi}) - \frac{\partial u_j(\bar{\xi})}{\partial \zeta_m} b_{mn} r_n \right] dS(\vec{x}) \tag{26}$$

$$+ \int_S T^*_{pj} dS(\vec{x}) u_j(\bar{\xi}) + \int_S T^*_{pj} r_n dS(\vec{x}) b_{mn} \frac{\partial u_j(\bar{\xi})}{\partial \zeta_m}$$

The second term of the right side in equation (26) is 0 by the identity(17). By applying the third kind identity(19)to equation(26), one obtains

$$\int_S T^*_{pj} u_j(\vec{x}) dS(\vec{x})$$

$$= \int_S T^*_{pj} \left[u_j(\vec{x}) - u_j(\bar{\xi}) - \frac{\partial u_j(\bar{\xi})}{\partial \zeta_m} b_{mn} r_n \right] dS(\vec{x}) \tag{27}$$

$$+ \int_S E_{iqjn} \left[U^*_{pi} n_q(\vec{x}) + T_{pi} v_q(\bar{\xi}) \right] dS(\vec{x}) b_{mn} \frac{\partial u_j(\bar{\xi})}{\partial \zeta_m}$$

By substituting equation (27) into equation(25), the following regularized traction representation is formed.

$$\int_S T^*_{pj} \left[u_j(\vec{x}) - u_j(\bar{\xi}) - \frac{\partial u_j(\bar{\xi})}{\partial \zeta_m} b_{mn} r_n \right] dS(\vec{x}) \tag{28}$$

$$+ \int_S E_{iqjn} \left[U^*_{pi} n_q(\vec{x}) + T_{pi} v_q(\bar{\xi}) \right] dS(\vec{x}) b_{mn} \frac{\partial u_j(\bar{\xi})}{\partial \zeta_m}$$

$$= \int_S \left[U^*_{pj} t_j(\vec{x}) + T_{pj} t_j(\bar{\xi}) \right] dS(\vec{x}) \quad \left(\bar{\xi} \in S \cup V, \vec{x} \in S \right)$$

By taking the limit $\bar{\xi} \to \vec{z}$, the source point $\vec{z}$ is moved to the boundary to form the regularized traction boundary integral equation.

$$\int_S T^*_{pj} \left[u_j(\vec{x}) - u_j(\vec{z}) - \frac{\partial u_j(\vec{z})}{\partial \zeta_m} b_{mn} r_n \right] dS(\vec{x}) \tag{29}$$

$$+ \int_S E_{iqjn} \left[U^*_{pi} n_q(\vec{x}) + T_{pi} v_q(\vec{z}) \right] dS(\vec{x}) b_{mn} \frac{\partial u_j(\vec{z})}{\partial \zeta_m}$$

$$= \int_S \left[U^*_{pj} t_j(\vec{x}) + T_{pj} t_j(\vec{z}) \right] dS(\vec{x}) \quad (\vec{x}, \vec{z} \in s)$$

All variables in equation(29)are now on the surface. Here, if α denotes the number of dimensions in Euclidean space, subscripts i, j, p, q and n take up to α value and m takes up to α-1 value. Now, by defining new vari-

able W_{pjm} as

$$W_{pjm} = E_{iqin}\left[U^*_{pi} n_q(\vec{x}) + T_{pi} v_q(\vec{z})\right] b_{mn} \qquad (30)$$

one has the following regularized traction boundary integral equation.

$$\int_S T^*_{pj}\left[u_j(\vec{x}) - u_j(\vec{z}) - \frac{\partial u_j(\vec{z})}{\partial \xi_m} b_{mn} r_n\right] dS(\vec{x}) + \int_S W_{pjm} dS(\vec{x}) \frac{\partial u_j(\vec{z})}{\partial \xi_m} = \int_S \left[U^*_{pj} t_j(\vec{x}) + T_{pj} t_j(\vec{z})\right] ds(\vec{x}) \qquad (\vec{x}, \vec{z} \in S) \qquad (31)$$

For the regularization by subtraction to be effective, one cannot use the TBIE's at points where the displacement derivatives are discontinuous, or, at the collocation point, the displacement must have continuous first derivatives. If a collocation point is located on the geometric end nodes in a 2-D or on the corner nodes in a 3-D element, the normal and the tangential vector components may not have unique values at common points for connected elements and one cannot construct the auxiliary surface for that collocation point. For these reasons, the TBIE's will be used only at collocation points which are located inside of boundary elements.

5. Computational Forms

For the computational and programming purposes, it is convenient to partition the whole integration range S into several parts, that is, $S = S' + S_o$ or $S = S' + S_o^+ + S_o^-$ where S_o is that part of the boundary containing the collocation point and S' is the remainder of S.

When the collocation point is on the crack surface, even though the collocation point is not on the integration element, the integration over the opposite crack surface becomes singular as $\bar{\xi}$ approach to $\bar{z}$. In this situation, one needs to partition the integration range into three parts, that is, $S = S' + S_o^+ + S_o^-$. Fig.2 shows schematic drawing for a cracked body. In the following, S_o^+ denotes one crack surface and S_o^- denotes the opposing crack surface. The DBIE's are collocated at points on the "+" side of the crack surface and the TBIE's are collocated at points on the "−" side of the crack.

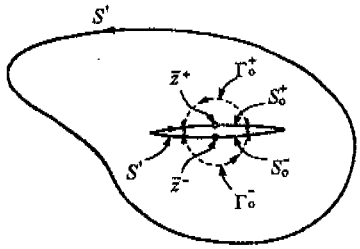

Fig. 2 Schematic drawing for a cracked body

When the collocation point is on the outer surface, the total boundary will be partitioned into two parts, that is, $S = S' + S_o$. Then, equation(23) with the identity(16) can be expressed as

$$\int_S T_{ij} u_j(\vec{x}) dS + \int_{S_o} T_{ij}[u_j(\vec{x}) - u_j(\vec{z})] dS - \int_{\Gamma_o} T_{ij} dS u_j(\vec{z}) = \int_{S'} U_{ij} t_j(\vec{x}) dS + \int_{S_o} U_{ij}[t_j(\vec{x}) - t_j(\vec{z})] dS + \int_{S_o} U_{ij} dS t_j(\vec{z}) \qquad (32)$$

On the crack surface, the total boundary will be partitioned into three parts, that is, $S = S' + S_o^+ + S_o^-$. With the partitioned integration ranges, the modified form of the first kind identity for the exterior(14) can be written as follows.

$$\int_{S'+S_o^+ + S_o^-} T_{ij} dS = 0 \qquad (33)$$

$$\int_{S'+S_o^-} T_{ij} dS = -\int_{S_o^+} T_{ij} dS \qquad (34)$$

By the use of the identity (34), the left side

of equation(23) can be written as

$$\int_{S'} T_{ij}u_j(\vec{x})dS + \int_{S_o^+} T_{ij}[u_j(\vec{x}) - u_j(\vec{z}^+)]dS + \int_{S_o^+} T_{ij}dSu_j(\vec{z}^+) + \int_{S_o^-} T_{ij}[u_j(\vec{x}) - u_j(\vec{z}^-)]dS + \int_{S_o^-} T_{ij}dSu_j(\vec{z}^-) \quad (35)$$

Here, one may introduce an auxiliary surface for the added back term integration through the modified form of the first kind identity for the exterior(15)for each crack surface.

$$\int_{S_o^+} T_{ij}dS = -\int_{\Gamma_o^+} T_{ij}dS \quad (36)$$

$$\int_{S_o^-} T_{ij}dS = -\int_{\Gamma_o^-} T_{ij}dS \quad (37)$$

Thus, one gets the computational form of the regularized DBIE's for the crack surface which has a form similar to equation for the outer surface(32).

$$\int_{S'} T_{ij}u_j(\vec{x})dS + \int_{S_o^+} T_{ij}[u_j(\vec{x}) - u_j(\vec{z}^+)dS - \int_{\Gamma_o^+} T_{ij}dSu_j(\vec{z}^+) + \int_{S_o^-} T_{ij}[u_j(\vec{x}) - u_j(\vec{z}^-)dS - \int_{\Gamma_o^-} T_{ij}dSu_j(\vec{z}^-) \quad (38)$$
$$= \int_{S'} U_{ij}t_j(\vec{x})dS + \int_{S_o^+} U_{ij}[t_j(\vec{x}) - t_j(\vec{z}^+)dS + \int_{S_o^+} U_{ij}dSt_j(\vec{z}^+) + \int_{S_o^-} U_{ij}[t_j(\vec{x}) - t_j(\vec{z}^-)dS + \int_{S_o^-} U_{ij}dSt_j(\vec{z}^-)$$

When one uses the TBIE's for the outer surface, the integration range is divided into two parts, $S=S'+S_o$. By applying identities, equatios (16) and (18), to the regularized TBIE's(31), one gets

$$\int_{S'} T_{Pj}^* u_j(\vec{x})dS - \int_{\Gamma_o} T_{Pj}^* dSu_j(\vec{z}) - \int_{\Gamma_o} T_{Pj}^* r_n dS \frac{\partial u_j(\vec{z})}{\partial \zeta_m} b_{mn} + \int_{\Gamma_o} W_{pjm}dS\frac{\partial u_j(\vec{z})}{\partial \zeta_m} + \int_{S_o} T_{pj}^*\left[u_j(\vec{x}) - u_j(\vec{z}) - \frac{\partial u_j(\vec{z})}{\partial \zeta_m} b_{mn}r_n\right]dS \quad (39)$$
$$+ \int_{S_o} W_{pjm}dS\frac{\partial u_j(\vec{z})}{\partial \zeta_m} = \int_{S'} U_{Pj}^* t_j(\vec{x})dS - \int_{\Gamma_o} T_{Pj}dSt_j(\vec{z}) + \int_{S_o} [U_{Pj}^- t_j(\vec{x}) + T_{pj}t_j(\vec{z})]dS$$

On the crack surface, the integration range is divided into three parts, that is, $S = S' + S_O^+ + S_O^-$. After several steps of equation rearrangement by applying the identities, one gets the computational form of the TBIE's on the crack surface at the point $\vec{z}^+$ which has a form similar to equation(39).

As mentioned in the previous, this TBIE has to be used only at points where the displacements have continuous first derivatives. If one uses the TBIE's for a collocation point on one crack surface, one should use the DBIE's for the point on the opposite crack surface to ensure a unique solution.

$$\int_{S'} T_{pj}^* u_j(\vec{x})dS - \int_{\Gamma_o^+} T_{pj}^* dSu_j(\vec{z}^+) - \int_{\Gamma_o^-} T_{pj}^* r_n dS \frac{\partial u_j(\vec{z}^+)}{\partial \zeta_m} b_{mn} + \int_{\Gamma_o^-} W_{pjm}dS\frac{\partial u_j(\vec{z}^+)}{\partial \zeta_m} + \int_{S_o^+} T_{pj}^*\left[u_j(\vec{x}) - u_j(\vec{z}^+) - \frac{\partial u_j(\vec{z}^+)}{\partial \zeta_m} b_{mn}r_n\right]dS + \int_{S_o^-} W_{pjm}dS\frac{\partial u_j(\vec{z}^+)}{\partial \zeta_m} - \int_{\Gamma_o^-} T_{pj}^* dSu_j(\vec{z}^-) \quad (40)$$
$$- \int_{\Gamma_o^-} T_{pj}^* r_n dS \frac{\partial u_j(\vec{z}^-)}{\partial \zeta_m} b_{mn} + \int_{\Gamma_o^-} W_{pjm}dS\frac{\partial u_j(\vec{z}^-)}{\partial \zeta_m} + \int_{S_o^-} T_{pj}^*\left[u_j(\vec{x}) - u_j(\vec{z}^-) - \frac{\partial u_j(\vec{z}^-)}{\partial \zeta_m} b_{mn}r_n\right]dS$$

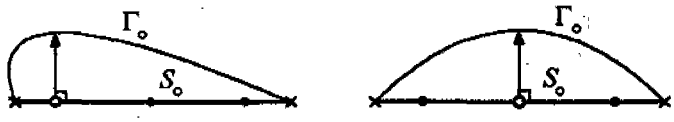

Fig. 3 An auxiliary surface on intrinsic element in a 2-D problem

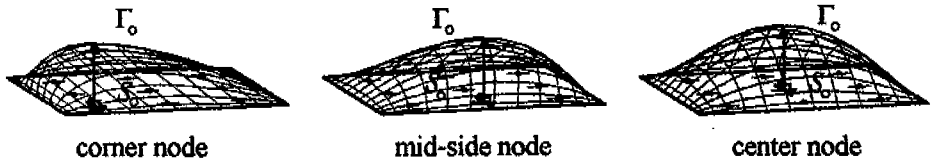

Fig. 4 An auxiliary surface on intrinsic element in a 3-D problem

$$+\int_{S_o^-} W_{pjm}\,dS\,\frac{\partial u_j(\vec{z}^-)}{\partial \zeta_m}$$
$$=\int_{S'} U^*_{pj} t_j(\vec{x})\,dS$$
$$+\int_{\Gamma_o^-} T_{pj}\,dS\,t_j(\vec{z}^+)+\int_{S_o^-}\left[U^*_{pj}t_j(\vec{x})+T_{pj}t_j(\vec{z}^+)\right]dS$$
$$-\int_{\Gamma_o^-} T_{pj}\,dS\,t_j(\vec{z}^-)+\int_{S_o^-}\left[U^*_{pj}t_j(\vec{x})-T_{pj}t_j(\vec{z}^-)\right]dS$$

6. Strong Singularity Integration by Use of the Auxiliary Surface

The added back integrals appearing after the regularization process are not singular even though they contain strongly singular fundamental solution kernels because the integration range does not include the element where the collocation points are positioned. When a crack exists and the collocation point is on one of the crack surfaces, the integration point is on the opposing crack surface element, then the integral is singular.

To remove stronger singularities, the actual surface containing the opposite crack surface is replaced by a smoothly curved auxiliary surface which isolates the singular integration path. The auxiliary surface can be any shape in the mathematical sense. The numerical integration over the auxiliary surface will have an ordinary value when the auxiliary surface is smooth, expecially for the traction boundary integral equations that the surface gradients are contained. For an optimal integration path for every singular collocation point, the auxiliary surface may have different shapes depending on the collocation point position on the singular element. One way of constructing the auxiliary surface is to displace the physical location of the collocation point in the opposite direction of the normal of the singular element at $\vec{z}$. The curved boundary is constructed by connecting geometric nodes and the relocated center point. The auxiliary surfaces on the intrinsic elements are shown in Fig. 3 and 4. By virtue of the constructed auxiliary surfaces, the added back integrals always have non-singular integration paths. Now, all integrals in the displacement and traction boundary integral equations are numerically integrable for both the outer and crack surfaces.

7. Computation of the Stress Intensity Factors

The stress intensity factors K_{I}, K_{II}, and K_{III} represent the strength of the stress field singularity at the crack tip. Each subscript of K denotes a mode of deformation. Term K_{I} is

related to the mode I deformation where the crack surface displacement is normal to the crack face and which tends to open the crack. K_I is related to in-plane shear deformation, that is, to slide one crack surface with respect to the other. K_{II} corresponds to out-of-plane shear. The stress intensity factors are determined by the crack geometry and the loads imposed but are not functions of the coordinates. In the examples, the stress intensity factors are computed from the displacement components by following approximate equations

$$\begin{bmatrix} K_I \\ K_{II} \\ K_{III} \end{bmatrix} = \begin{bmatrix} \Delta u_n \\ \Delta u_t \\ \Delta u_s(1+\nu) \end{bmatrix} \sqrt{\frac{\pi}{2}} \frac{E}{4(1-\nu^2)} \cdot \frac{1}{\sqrt{r}} \qquad (41)$$

where r is the distance from the crack tip to the stress intensity factor computing point. The variable Δu indicates the crack opening displacement at each point and the subscript n is for the component normal to the crack surface and t and s are the tangent components, respectively. In the examples, the stress intensity factor is determined from the nodal displacement components, near the crack tip point which is on the crack front element in 2-D and at the center of the crack front element in 3-D problems. Then, the computed stress intensity factors are normalized and compared to analytic or empirical solutions.

8. Numerical Examples

To evaluate and check the presented formulations, each one of typical 2-D and 3-D mixed-mode crack problem was simulated. Both sides of the crack surfaces are modelled with discontinuous elements and the TBIE's are collocated at points on one crack surface while the DBIE's are collocated at points on the opposite surface.

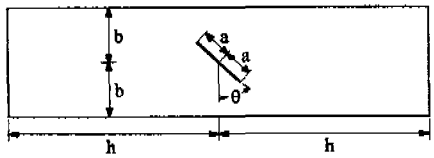

Fig. 5 A centered slant crack in a finite plate

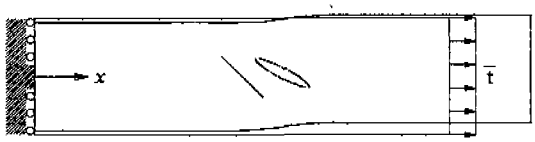

Fig. 6 Initial and deformed shape of a centered 45° slant crack in a rectangular plate subjected to tension(h/b=3.5, a/b=0.5)

Table 1 $< K_I >= \frac{K_I}{\sigma\sqrt{\pi a}}$ and $< K_{II} >= \frac{K_{II}}{\sigma\sqrt{\pi a}}$ for a centered 45° slant crack in a rectangular plate

a/b[a]	$\langle K_I \rangle$[b]	$\langle K_I \rangle$[a]	% error	$\langle K_{II} \rangle$[b]	$\langle K_{II} \rangle$[c]	% error
0.1	0.505	0.517	+2.38	0.502	0.515	+2.59
0.2	0.518	0.532	+2.70	0.507	0.520	+2.56
0.3	0.541	0.555	+2.59	0.516	0.529	+2.52
0.4	0.572	0.589	+2.97	0.529	0.541	+2.27
0.5	0.612	0.632	+3.27	0.546	0.558	+2.20
0.6	0.661	0.687	+3.93	0.567	0.578	+1.94
0.7	0.721	0.755	+4.72	0.595	0.604	+1.51
0.8	0.795	0.841	+5.79	0.630	0.635	+0.79

a. See Fig. 5 for the ratio of a crack length to the plate width.
b. Murakami[22](p.911).
c. by the BEM: 38-elements on the outer surfaces, 9-elements on each crack surface.

In two-dimensional crack problem, a centered 45° slant cracked plate was chosen. Analyzed crack length to plate width ratios are a/b=0.1, 0.2, 0.3, ···, 0.8, where a denotes one-half of the crack length and b denotes one-half of the plate width as shown in Fig. 5. Fig. 6 shows the initial and the deformed shapes of the analyzed model subjected to tension. The center part of the left end is fixed in both degrees of freedom and a uniform tensile load is applied at the other end to the x-direction. The stress intensity factors, both of the opening mode K_I and the in-plane shear mode K_{II}, are given tn Table 1.

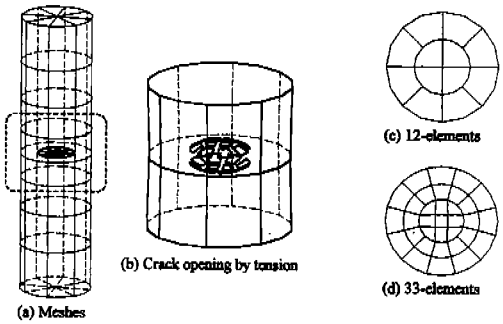

Fig. 7 A penny-shaped crack in a solid cylinder (a/b=0.5)

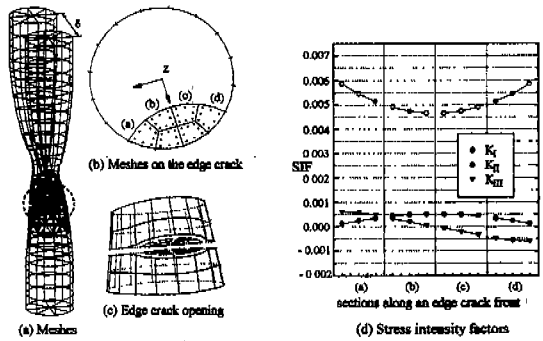

Fig. 8 An hourglass-shaped bar with an edge crack

Table 2 $< K_I >= \frac{K_I}{\sigma_{net}\sqrt{\pi a}}$ and $< K_{III} >= \frac{K_{III}}{\tau_{net}\sqrt{\pi a}}$ for a penney-shaped crack in a solid cylinder

a/b[a]	$\langle K_I \rangle$[b]	$\langle K_I \rangle$[c]	% error	$\langle K_{III} \rangle$[d]	$\langle K_{III} \rangle$[e]	% error
0.05	0.635	0.621	-2.20	0.424	0.437	+3.07
0.1	0.631	0.630	-0.16	0.424	0.437	+3.07
0.2	0.614	0.616	+0.33	0.424	0.437	+3.07
0.3	0.589	0.591	+0.34	0.421	0.434	+3.09
0.4	0.556	0.557	+0.18	0.415	0.428	+3.13
0.5	0.516	0.517	+0.19	0.402	0.414	+2.99
0.6	0.469	0.469	0.0	0.379	0.391	+3.17
0.7	0.414	0.413	-0.24	0.342	0.355	+3.80
0.8	0.346	0.346	0.0	0.288	0.298	+3.47
0.9	0.252	0.256	+1.59	0.205	0.205	0.0

a. Ratio of the centered penny-shaped crack radius to the cylinder outer radius.
b. Tada[23](p.28.1).
c. by the BEM, see Fig. 7(d) for used meshes on one crack surface.
d. Tada[23](p.28.3).
e. by the BEM, see Fig. 7(c) for used meshes on one crack surface.

In three dimensional crack problems, a penny-shaped crack embedded in a cylindrical bar under tension or under torsion was analyzed. Before solving the problem of a cylindrial bar with an embedded penny-shaped crack, a solid cylinder model without a crack is first prepared and solved. Total 80-elements were used on the outer surfaces of the cylinder. By adding the mesh for a penny-shaped crack shown in Fig. 7(c) or Fig. 7(d) to the solid cylinder model, the mesh for the crack problem is completed. The bottom surface of the cylinder is fixed. Uniform traction for K_I mode or torsion for K_{II} mode was applied to the top surface. Analyzed ratios of crack radius to the cylinder outer radii are a/b=0.05, 0.1, 0.2, ···, 0.9, where a denotes the crack radius and b denotes the cylinder outer radius. The meshes and the zoomed out deformed shape of the crack portion for the case a/b=0.5 are shown in Fig. 7(a) and (b), respectively. The calculated stress intensity factors K_I and K_{II} are given in Table 2.

As the last example, an hourglass shaped bar with an edge crack was analyzed as a practical application. The lower part of the bar is fixed and the upper part is deflected. On the outer surfaces, 224 quadrilateral and 64 triangular quadratic elements were used(Fig. 8(a)). On each crack surface, 6 quadrilateral quadratic elements were used as shown in Fig. 8(b). The opened crack shape caused by the deflection of the upper end is shown in Fig. 8(c). An hourglass shaped bar model has three deformation modes. The opening mode K_I and the in-plane shear mode K_{II} are symmetric and the shear mode K_{III} is anti symmetric with respect to the center of the crack front. The calculated stress intensity factors for three different modes are given in

Fig. 8(d).

9. Conclusions

A dual boundary integral equation method for a single-region solution of a general mixed-mode crack in two- and three-dimensional elastostatics has been developed. The displacement and the traction boundary integral equations were developed by taking the limit of the relevant representation equations. Modified integral identities were developed from the formal integral identities by using auxiliary surfaces. The strongly singular and the hypersingular integrals in the displacement and the traction boundary integral equations, respectively, are regularized using the key terms of the Taylor expansion of the displacement functions and the identities pertaining to the fundamental solutions.

To isolate the added back, strongly singular integrals, surface elements containing the collocation point and the opposing crack surface elements are replaced by auxiliary surfaces which provide non-singular integration paths. On the crack surfaces, discontinuous quadrilateral elements were used to satisfy the continuity requirement. The traction boundary integral equations are collocated at points on one crack surface while the displacement boundary integral equations are collocated at points on the opposite crack surface. When the crack shape changes, the developed method requires mesh modifications only on the crack surface.

Convergence tests for the introduced auxiliary surfaces show that the stress intensity factors are not sensitive to the number of elements on the auxiliary surface but do depend on the integration order for elements on curved outer surfaces. Numerical analysis for two- and three-dimensional mixed mode crack shows fairly accurate results in stress intensity factors calculation.

In conclusion, one may note that the present formulation and the solution method would be readily applicable to many areas in fracture mechanics including the analysis of general mixed-mode crack problems and crack growth by the fatigue loading.

References

1. Crouch, S. L., Solution of Plane Elasticity Problems by the Displacement Discontinuity Method, *Int. J. Numer. Meth. Eng.*, 10, pp.301-343, 1976.
2. Cruse, T. A., Two-dimensional BIE fracture mechanics analysis, *Appl. Math. Modelling*, 2, pp.287-293, 1978.
3. Blandford, G. E., Ingraffea, A. R. and Liggett, J. A., Two-Dimensional Stress Intensity Factor Computations Using the Boundary Element Method, *Int. J. Numer. Meth. Eng.*, 17, pp.387-404, 1981.
4. Hong, H. K. and Chen, J. T., Derivations of Integral Equations of Elasticity, *J. Eng. Mech. ASCE*, 114, pp.1028-1044, 1988.
5. Guidera, J. T. and Lardner, R. W., Penny-shaped Cracks, *J. Elast.*, 5(1), pp.59-73, 1975.
6. Cruse, T. A. and Vanburen, W., Three-Dimensional Elastic Stress Analysis of a Fracture Specimen with an Edge Crack, *Int. J. Fract. Mech.*, 7(1), pp.1-15, 1971.
7. Jeng, G. and Wexler, A., Isoparametric, Finite Element, Variational Solution of Integral Equations for Three-Dimensional Fields, *Int. J. Numer. Meth. Eng.*, 11, pp.1455-1471, 1977.
8. Aliabadi, M. H., Hall, W. S. and Phemister, T. G., Taylor Expansions for

Singular Kernels in the Boundary Element Method, *Int. J. Numer. Meth. Eng.*, 21, pp.2221-2236, 1985.

9. Brandao, M. P., Improper Integrals in Theoretical Aerodynamics: The Problem Revisited, *AIAA J.*, 25(9), pp.1258-1260, 1986.
10. Kaya, A. C. and Erdogan, F., On the Solution of Integral Equations with Strongly Singular Kernels, *Quart. Appl. Math.*, XLV(1), 105-122, 1987.
11. Krishnasamy, G., Schmerr, L. W., Rudolphi, T. J. and Rizzo, F. J., Hypersingular Boundary Integral Equations: Some Applications in Acoustics and Elastic Wave Scattering, *J. Appl. Mech.*, 57, pp.404-414, 1990.
12. Rudolphi, T. J. and Muci-Kuchler, K. H., Consistent Regularization of Both Kernels in Hypersingular Integral Equations, in Boundary Elements XIII, Edited by Brebbia, C. A. and Gipson, G. S., *Proceedings of the Boundary Elements XIII Conference*, Tulsa, Oklahoma, August 21-23, 1991, CMP, Elsevier, Southampton, pp.875-887, 1991.
13. Ioakimidis, N. I., Two-Dimensional Principal Value Hypersingular Integrals for Crack Problems in Three-Dimensional Elasticity, *Acta Mechanica*, 82, pp.129-134, 1990.
14. Gray, L. J., Martha, L. F. and Ingraffea, A. R., Hypersingular Integrals in Boundary Element Fracture Analysis, *Int. J. Numer. Meth. Eng.*, 29, pp.1135-1158, 1990.
15. Guiggiani, M., Krishnasamy, G., Rudolphi, T. J. and Rizzo, F. J., A General Algorithm for the Numerical Solution of Hypersingular Boundary Integral Equations, *Trans. ASME*, 59, pp.604-614, 1992.
16. Rudolphi, T. J., The use of Simple Solutions in the Regularization of Hypersingular Boundary Integral Equations, *Mathl. Comput. Modelling*, 15(3-5), pp.269-278, 1991.
17. Liu, Y. and Rudolphi, T. J., Some Identities for Fundamental Solutions and Their Applications to Non-Singular Boundary Element Formulations, *Eng. Anal. with Bound. Elem.*, 8(6), pp.301-311. 1991.
18. Lutz, E., Gray, L. J. and Ingraffea, A. R., An Overview of Integration Methods for Hypersingular Boundary Integrals, in Boundary Elements XIII, Edited by Brebbia, C. A. and Gipson, G. S., *Proceedings of the Boundary elements XIII Conference*, Tulsa, Oklahoma, August 21-23, CMP, Elsevier, Southampton, pp.913-925, 1991.
19. Portela, A., Aliabadi, M. H. and Rooke, D. P., The Dual Boundary Element Method: Effective Implementation for Crack Problems, *Int. J. Numer. Meth. Eng.*, 33, pp. 1269-1287, 1992.
20. Mi, Y. and Aliabadi, M. H., Dual Boundary Element Method for Three-Dimensional Fracture Mechanics Analysis, *Eng. Anal. with Bound. Elem.*, 10, pp.161-171, 1992.
21. Youn, S., *Application of Displacement and Traction Boundary Integral Equations for Fracture Mechanics Analysis*, Ph. D. thesis, Iowa State University, Ames, Iowa, 1993.
22. Murakami, Y., et al., *Stress Intensity Factors Handbook*, Pergamon Press, Oxford, 1987.
23. Tada, H., Paris, P. C. and Irwin, G. R., *The Stress Analysis of Cracks Handbook*, Del Research Corporation, Hellertown, 1973.